J|A|C|S
A R T I C L E S

Solid-State Packing of Conjugated Oligomers: From π-Stacks to the Herringbone Structure

M. David Curtis,* Jie Cao, and Jeff W. Kampf

Contribution from the Department of Chemistry, and the Macromolecular Science and Engineering Program, The University of Michigan, Ann Arbor, Michigan 48109-1055

Received November 25, 2003; E-mail: mdcurtis@umich.edu

Abstract: The solid-state structures of a series of bithiazole and thiophene oligomers, as well as a series of substituted pentacenes, are rationalized in terms of "pitch and roll" inclinations from an "ideal" cofacial π-stack. Pitch inclinations translate adjacent molecules relative to one another in the direction of the long molecular axis, whereas roll inclinations translate the molecules along the short molecular axis. Thus, moderately large pitch distortions preserve $\pi-\pi$ interactions between adjacent molecules, whereas roll translations greater than 2.5 Å essentially destroy $\pi-\pi$ overlap between adjacent molecules. The familiar herringbone packing is characterized by large roll distortions. It is shown that thiophenes tend to exhibit large roll translations, whereas thiazoles have small roll but large pitch translations. Substituted pentacenes tend to have both moderate pitch and roll distances. The relationship of molecular packing to transport properties is discussed.

Introduction

The solid-state morphology of conjugated polymers plays an important role in the performance characteristics of electronic devices, e.g., organic light-emitting diodes (OLEDs)[1-6] and organic thin-film transistors (OTFTs).[7-11] Both exciton migration and carrier mobility are strongly modulated by the solid-state packing of the conjugated chains. In particular, increased *intermolecular* overlap of electronic wave functions leads to increased bandwidth, which is directly related to carrier mobility in the coherent transport regime.[12-17] For a one-dimensional chain, the bandwidth is given by $W = 4J$, where J is the nearest-neighbor intermolecular $\pi-\pi$ coupling $= \int \psi_u V_{int} \psi_v d\tau$.[12,13] If transport occurs via a hopping mechanism, then the hopping rate constant is also increased by decreased distance and increased overlap of electron density between neighboring molecules. Similarly, the exciton band structure is governed by the signs and magnitudes of intermolecular dipolar coupling, which, in turn, are determined by the relative positions of nearby molecules and their transition dipole moments.[18,19] The position of the $k = 0$ level, if at the top or bottom of the exciton band, determines whether a material is suitable for application in an OLED or organic laser.

Structural analysis of some popular OTFT materials, e.g., pentacene and sexithiophene, has shown that the crystal structures of all these molecules share the so-called "herringbone" motif in which the molecules are packed more or less edge-to-face in two-dimensional (2-D) layers.[20-22] Although the highest mobilities are in the 2-D layers,[23-25] the edge-to-

(1) Nalwa, H. S. *Handbook of Advanced Electronic and Photonic Materials and Devices*; Academic Press: 2001.
(2) Lo, S. C.; Male, N. A. H.; Markham, J. P. J.; Magennis, S. W.; Burn, P. L.; Salata, O. V.; Samuel, I. D. W. *Adv. Mater.* **2002**, *14*, 975.
(3) Schott, M. *C. R. Acad. Sci. Ser. IV: Phys. Astrophys.* **2000**, *1*, 381.
(4) Mitschke, U.; Bäuerle, P. *J. Mater. Chem.* **2000**, *10*, 1471.
(5) Hudson, A. J.; Weaver, M. S. *Organic Electroluminescence*; John Wiley & Sons: New York, 2000.
(6) Bao, Z. N.; Rogers, J. A.; Dodabalapur, A.; Lovinger, A. J.; Katz, H. E.; Raju, V. R.; Peng, Z.; Galvin, M. E. *Opt. Mater.* **1999**, *12*, 177.
(7) Dimitrakopoulos, C. D.; Malenfant, P. R. L. *Adv. Mater.* **2002**, *14*, 99.
(8) Katz, H. E.; Bao, Z. *J. Phys. Chem. B* **2000**, *104*, 671.
(9) Horowitz, G. *J. Mater. Chem.* **1999**, *9*, 2021.
(10) Horowitz, G. *Adv. Mater.* **1998**, *10*, 365.
(11) Lovinger, A. J.; Rothberg, L. J. *J. Mater. Res.* **1996**, *11*, 1581.
(12) Kittel, C. *Introduction to Solid State Physics*, 7th ed.; John Wiley & Sons: New York, 1996.
(13) Pope, M.; Swenberg, C. E. *Electronic Processes in Organic Crystals and Polymers*, 2nd ed.; Oxford University Press: 1999.
(14) Brédas, J. L.; Beljonne, D.; Cornil, J.; Calbert, J. P.; Shuai, Z.; Silbey, R. *Synth. Met.* **2001**, *125*, 107.
(15) Cornil, J.; Beljonne, D.; Calbert, J. P.; Bredas, J. L. *Adv. Mater.* **2001**, *13*, 1053.
(16) (a) Pappenfus, T. M.; Chesterfield, R. J.; Frisbie, C. D.; Mann, K. R.; Casado, J.; Raff, J. D.; Miller, L. L. *J. Am. Chem. Soc.* **2002**, *124*, 4184. (b) Chesterfield, R. J.; Newman, C. R.; Pappenfus, T. M.; Ewbank, P. C.; Haukaas, M. H.; Mann, K. R.; Miller, L. L.; Frisbie, C. D. *Adv. Mater.* **2003**, *15*, 1278. (c) Pappenfus, T. M.; Raff, J. D.; Hukkanen, E. J.; Burney, J. R.; Casado, J.; Drew, S. M.; Miller, L. L.; Mann, K. R. *J. Org. Chem.* **2002**, *67*, 6015.
(17) Li, X. C.; Sirringhaus, H.; Garnier, F.; Holmes, A. B.; Moratti, S. C.; Feeder, N.; Clegg, W.; Teat, S. J.; Friend, R. H. *J. Am. Chem. Soc.* **1998**, *120*, 2206.
(18) (a) McRae, E. G.; Kasha, M. In *Physical Processes in Radiation Biology*; Augenstein, L., Mason, R., Rosenberg, B., Ed.; Academic Press: New York, 1964; Chapter 8. (b) Giacintov, N. E.; Swenberg, C. E. In *Luminescence Spectroscopy*; Lumb, M. D., Ed.; Academic Press: New York, 1978; p 239ff. (c) Broude, V. L.; Rashba, E. I.; Sheka, E. F. Spectroscopy of Molecular Excitons. In *Springer Series in Chemical Physics 16*; Goldanskii, V. I., Ed.; Springer-Verlag: New York, 1985. (d) Rebane, K. K. *Impurity Spectra of Solids, Elementary Theory of Vibrational Structure*; Scheir, J. S., trans.; Plenum Press: New York, 1970. (e) Kasha, M. *Radiation Res.* **1963**, *20*, 55.
(19) Koren, A. B.; Curtis, M. D.; Francis, A. H.; Kampf, J. W. *J. Am. Chem. Soc.* **2003**, *125*, 5040.
(20) Holmes, D.; Kumaraswamy, S.; Matzger, A. J.; Vollhardt, K. P. C. *Chem. Eur. J.* **1999**, *5*, 3399.
(21) Horowitz, G.; Bachet, B.; Yassar, A.; Lang, P.; Demanze, F.; Fave, J. L.; Garnier, F. *Chem. Mater.* **1995**, *7*, 1337.
(22) Siegrist, T.; Fleming, R. M.; Haddon, R. C.; Laudise, R. A.; Lovinger, A. J.; Katz, H. E.; Bridenbaugh, P.; Davis, D. D. *J. Mater. Res.* **1995**, *10*, 2170.
(23) Sirringhaus, H.; Brown, P. J.; Friend, R. H.; Nielsen, M. M.; Bechgaard, K.; Langeveld-Voss, B. M. W.; Spiering, A. J. H.; Janssen, R. A. J.; Meijer, E. W.; Herwig, P.; de Leeuw, D. M. *Nature* **1999**, *401*, 685.
(24) Osterbacka, R.; An, C. P.; Jiang, X. M.; Vardeny, Z. V. *Science* **2000**, *287*, 839.
(25) Lee, K.; Heeger, A. J. *Synth. Met.* **2002**, *128*, 279.

Scheme 1
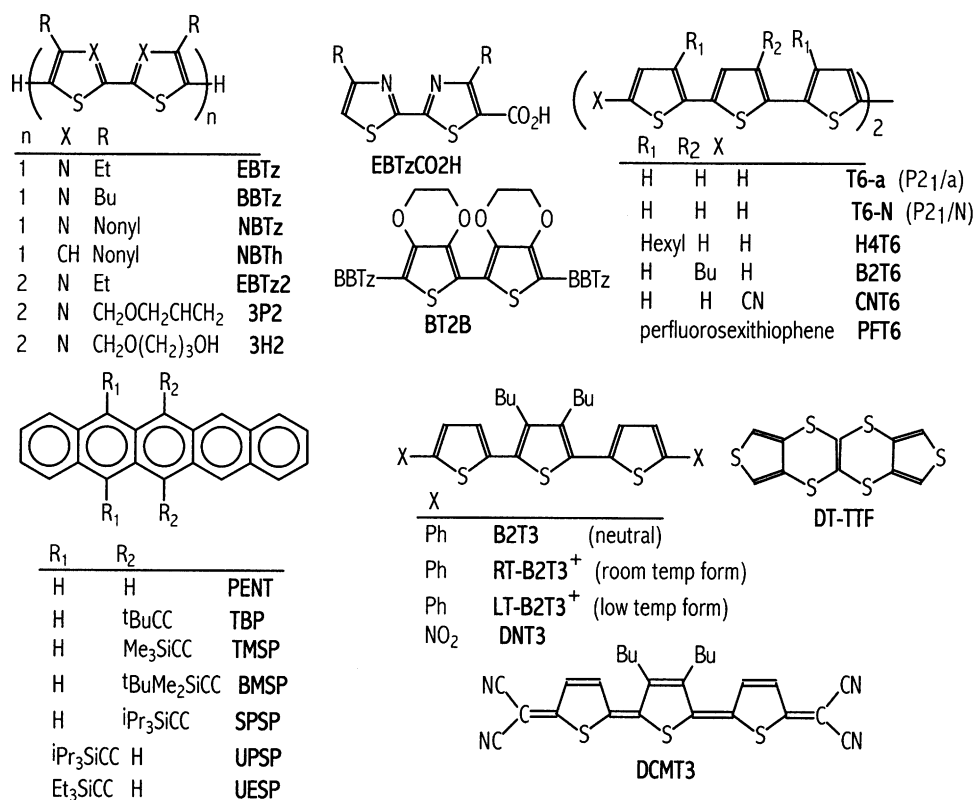
face packing minimizes π–π overlap between adjacent molecules. As a result, higher mobilities at room temperature might be achieved by designing conjugated molecules that stack face-to-face (π-stack) in the solid state, thus increasing the intermolecular interaction, while maintaining the desirable 2-D character of the herringbone structure.[14–17] In addition to having a 2-D π-stacked morphology, the ideal OTFT material would self-assemble on the surface of a substrate, e.g., the insulating layer of an OTFT gate, such that the π-stacks would be parallel to the surface, i.e., the direction of highest mobility would coincide with the direction of current flow in the OTFT.[24,26,27]

The presence of π-stacks may often be inferred from X-ray diffraction patterns. The π-stacking distance is typically 3.4–3.6 Å, representing the shortest interplanar distance.[19,28,29] However, detailed characterizations of π-stacking structures are rare because of the relative scarcity of π-stacked materials and the difficulty of growing single crystals. In this paper, the structures of several alkylbithiaozle and bithiophene oligomers are reported for the first time. The side-chains include ethyl, butyl, or nonyl groups. The carboxylic acid group was selectively introduced at the 5-position of some oligomers to study its effect on solid-state packing. These crystal structures, along with those of other conjugated oligomers used in electronic applications, are compared using a phenomenological approach that describes angular and lateral deviations from an "ideal",

cofacial π-stack. Here, our emphasis is on the solid-state packing motifs rather than the details of the internal molecular structures.

Experimental Section

Syntheses of the alkylbithiazole monomers and oligomers have been, or will be, reported elsewhere.[19,30–34] Abbreviations used in this paper are linked with their structures in Scheme 1, and the systematic names are as follows: **NBTz**, 4,4′-dinonyl-2,2′-bithiazole;[32] **NBTh**, 4,4′-dinonyl-2,2′-bithiophene;[33] **EBTz**, 4,4′-diethyl-2,2′-bithiazole; **EBTz-CO₂H**, 5-carboxy-4,4′-diethyl-2,2′-bithiazole; **EBTz2**, 4,4′,4″,4‴-tetraethyl-2,2′,5,5′,2″,2‴-quaterthiaozle, i.e., the dimer of EBTz, coupled at the 5′,5″-position; **3P2** and **3H2** (4,4′,4″,4‴-tetra"alkyl"-2,2′,5,5′,2″,2‴-quaterthiaozle with "alkyl" being 3-propenoxymethyl and 3-hydroxypropanoxymethyl, respectively);[19] **BT₂B**, 5,5′-bis(4,4′-dibutyl-2,2′-bithiazol-5-yl)-(3,4,3′,4′-bis(ethylenedioxy)-2,2′-dithienyl);[30] **BBD**, 1,4-bis(4,4′-dialkyl-2,2′-bithiazol-5-yl)-1,3-butadiyne;[34] **DT-TTF**, 2,2′-bithieno(3,4-*d*)-1,3-dithiole ("dithiophene-tetrathiafulvalene").[35] The structures of these compounds are shown in Scheme 1. The crystal data on all the other compounds listed in Scheme 1 and Tables 3–5 were obtained from the Cambridge Crystallographic Data Center.

Brief reports of the crystal structures of **NBTz**, **3P2**, **3H2**, and **BBD** have appeared previously.[19,32,34] The structures of **NBTh**, **EBTz**, **EBTz-COOH**, **EBTz2**, and **BT₂B** are reported here for the first time. Crystals were grown using the slow evaporation technique.[36] Crystallographic information files (CIF) are provided in Supporting Information. Crystal structures were visualized and the "pitch" and "roll" angles (see below)

(26) Hu, W. P.; Liu, Y. Q.; Xu, Y.; Liu, S. G.; Zhou, S. Q.; Zhu, D. B. *Synth. Met.* **1999**, *104*, 19.

(27) Reitzel, N.; Greve, D. R.; Kjaer, K.; Hows, P. B.; Jayaraman, M.; Savoy, S.; McCullough, R. D.; McDevitt, J. T.; Bjornholm, T. *J. Am. Chem. Soc.* **2000**, *122*, 5788.

(28) Yamamoto, T.; Komarudin, D.; Arai, M.; Lee, B. L.; Suganuma, H.; Asakawa, N.; Inoue, Y.; Kubota, K.; Sasaki, S.; Fukuda, T.; Matsuda, H. *J. Am. Chem. Soc.* **1998**, *120*, 2047.

(29) Politis, J. K.; Nemes, J. C.; Curtis, M. D. *J. Am. Chem. Soc.* **2001**, *123*, 2537.

(30) Cao, J.; Kampf, J. W.; Curtis, M. D. *Chem. Mater.* **2003**, *15*, 404.

(31) Cao, J.; Curtis, M. D. Submitted for publication.

(32) Nanos, J. I.; Kampf, J. W.; Curtis, M. D. *Chem. Mater.* **1995**, *7*, 2232.

(33) Brukwicki, M. P., Ph.D. Thesis, University of Michigan, Ann Arbor, MI, 2001, p 30 (via modification of the method reported in: Zagorska, M.; Krische, B. *Polymer* **1990**, *31*, 1379).

(34) Lee, J.-H.; Curtis, M. D.; Kampf, J. W. *Macromolecules* **2000**, *33*, 2136.

(35) C.Rovira, C.; Veciana, J.; Santalo, N.; Tarres, J.; Cirujeda, J.; Molins, E.; Llorca, J.; Espinosa, E. *J. Org. Chem.* **1994**, *59*, 3307.

(36) Jones, P. G. *Chem. Ber.* **1981**, *17*, 222.

Table 1. Summary of Crystallographic and Refinement Data for Bithiazole and Bithiophene Oligomers[a]

crystal	**EBTz**	**EBTz-COOH**	**EBTz2**	**BT$_2$B**	**NBTh**
space group	$P_{2(1)/n}$	$C_{2/c}$	$C_{2/c}$	$P_{2(1)/n}$	$P_{2(1)/c}$
unit cell	$a = 5.208$	$a = 22.664$	$a = 22.497$	$a = 14.517$	$a = 16.161$
(a,b,c: Å)	$b = 10.340$	$b = 5.188$	$b = 5.314$	$b = 9.701$	$b = 4.977$
	$c = 10.018$	$c = 22.754$	$c = 18.597$	$c = 16.816$	$c = 15.218$
($\alpha,\gamma = 90°$)	$\beta = 98.330°$	$\beta = 113.443°$	$\beta = 111.039°$	$\beta = 99.820°$	$\beta = 100.91°$
Z	2	8	4	2	2
density (Mg/m^3)	1.396	1.452	1.43	1.436	1.157
data range (θ)	2.85−26.38	3.27−27.15	1.94−26.39	1.71−26.42	2.57−26.5
data/restraints/parameters	1093/0/89	2720/0/203	2130/0/172	4771/1/297	2474/0/213
GOF on F^2	1.106	1.034	1.074	1.044	1.076
R_1 (all data)	0.0251	0.0382	0.0391	0.0529	0.0317
wR_2 (all data)	0.0637	0.0771	0.0841	0.1035	0.0826

[a] All refinements were on F^2.

Table 2. Pitch and Roll Angles and Distances for Bithiazole-Containing Oligomers

	P	R		d	d_p	d_r	d_{tot}	z	
compd	(deg)	(deg)	N	(Å)	(Å)	(Å)	(Å)	(Å)[a]	Δ%
NBTz	41.5	14.3	42.6	3.45	3.05	0.88	3.17	4.69 (b)	0.8
EBTz	42.6	21.9	45.1	3.67	3.37	1.47	3.68	5.18 (a)	0.5
3P2	39	25.7	43.3	3.46	2.80	1.67	3.26	4.75 (a)	0.6
3H2	44.1	23.0	46.6	3.41	3.30	1.45	3.60	4.96 (a)	0.6
EBTz2	48	12.1	48.5	3.47	3.86	0.75	3.93	5.26 (b)	1.0
EBTzCO2H	47.3	15.4	48.2	3.42	3.71	0.94	3.83	5.13 (b)	1.0
BT$_2$B	69.0	8.16	69.0	3.50	9.25	0.51	9.26	9.76 (b)	0.6
BBD	45.5	12.1	46.1	3.58	3.64	0.77	3.72	5.16 (b)	0.6
av[b]	44.4	17.8	45.6	3.49	3.39	1.13	3.60		

[a] Letter in parentheses represents the crystallographic stacking axis. [b] Average values exclude those for **BT$_2$B**.

Table 3. Pitch and Roll Angles and Distances for Thiophene-Containing Oligomers

	P	R		d	d_p	d_r		z	
compd	(deg)	(deg)	N	(Å)	(Å)	(Å)	d_{tot}	(Å)[a]	Δ%
NBTh	2.6	47.9	48.1	3.36	0.15	3.72	3.72	5.01 (b)	0.6
B2T3	38.0	53.5	57.5	3.19	2.49	4.32	4.99	5.92 (c)	0.5
T6-a	0.0	60.7	60.9	2.79	0.0	4.98	4.98	5.71 (b)	0.5
T6-n	41.3	58.4	61.7	2.85	2.50	4.64	5.27	5.99 (c)	0.7
H4T6	33.9	44.0	49.7	3.57	2.40	3.45	4.20	5.51 (a)	0.4
B2T6	2.08	61.54	61.7	2.76	0.10	4.90	4.90	5.62 (b)	0.5
CNT6	6.50	68.0	68.2	2.20	0.25	5.45	5.46	5.88 (b)	0.5
PFT6	47.5	21.3	49.2	3.48	3.80	1.36	4.04	5.33 (b)	0.1
DT-TTF	1.92	26.0	49.4	3.58	0.12	1.75	1.75	3.99 (b)	0.1
av	19.0	48.6	54.0	3.03	1.31	3.79	4.37		

[a] Calculated crystallographic stacking axis. Letter in parentheses represents the crystallographic stacking axis.

Table 4. Pitch, Roll, and Yaw Angles and Distances for Various Pentacenes

	P	R		d	d_p	d_r	d_{tot}	z	
compd	(deg)	(deg)	N	(Å)	(Å)	(Å)	(Å)	(Å)[a]	Δ%
PENT	39.1	64.2	65.8	2.58	2.10	5.35	5.75	6.30 (a)	0.4
TBP	58.6	14.8	58.9	3.34	5.48	0.87	5.55	6.48 (b)	0.1
TMSP	53.0	18.8	53.9	3.43	4.55	1.17	4.70	5.82 (a)	0.3
av	50.2	32.6	59.6	3.12	4.04	1.02[b]	5.33		

[a] Letter in parentheses represents the crystallographic stacking axis. (b) Excludes the value for **PENT**.

were measured with the programs Mercury, Cerius 2 (version 4.2), Spartan02, or Cache 5.0. A summary of the previously unreported crystallographic results for the bithiazole oligomers and **NBTh** are collected in Table 1.

Results

Conjugated oligomers usually adopt a planar or near-planar conformation in the solid state because planar molecules can be packed more densely than the twisted or nonplanar conformations. The detailed packing arrangement depends, inter alia, on the nature of the main chain,[29,37] the presence or absence of side chains, and their nature (branched or linear) and their position of attachment (regioregularity). Regioregular polymers are usually semicrystalline, and the packing in the crystalline region often resembles that seen in corresponding oligomers.[38,39] Thus, studies of the solid-state packing of conjugated oligomers is not only important in understanding the performance of electronic devices based on oligomers but is relevant to understanding polymer properties as well.[39]

Planar, conjugated oligomers typically have a large aspect ratio, i.e., their length is greater than their width or thickness. The thickness may be slightly altered by the nature of the main chain,[29] but, as a general rule, a value near 3.4−3.6 Å is typical for the $\pi-\pi$ contact distance in organic materials. The width of aromatic or heteroaromatic rings is roughly 3 Å. The length depends on the degree of oligomerization, n, and is about $n \times$ width for polyphenylenes or polythiophenes, etc.

It is well recognized, of course, that the nature of the side chains, if present, greatly affects the solid-state packing of conjugated oligomers and polymers.[39a,40] If side chains are absent, e.g., in oligo-acenes, -thiophenes, or -phenylenes, the usual packing morphology is the so-called "herringbone" structure, exemplified by the view down the long axis of pentacene as shown in Figure 1.[20] If linear alkyl side chains are present, crystallization of the side chains promotes the "lamellar" structure, an example of which is shown in Figure 4. In the lamellar structure, the conjugated main chains are forced into in a π-stacked, more cofacial arrangement. The direct, on-top, or cofacial stacking of π-systems is not energetically favorable at relatively close (ca. 3.5 Å) intermolecular distances because this structure places regions of like electron density on adjacent molecules into close proximity. To alleviate these unfavorable electrostatic interactions, the π-stacks distort away from the "ideal" on-top stacking motif.

The inclinations in a given π-stack may be described by two angles, which we call "pitch" (P) and "roll" (R) in analogy with

(37) Politis, J. K.; Somoza, F. B., Jr.; Kampf, J. W.; Curtis, M. D.; Gonzalez Ronda, L.; Martin, D. C. *Chem. Mater.* **1999**, *11*, 2274.
(38) Gonzalez-Ronda, L.; Martin, D. C.; Nanos, J.; Politis, J. K.; Curtis, M. D *Macromolecules* **1999**, *32*, 4558.
(39) (a) Müller, K.; Wegner, G. *Electronic Materials: The Oligomer Approach*; Wiley-VCH: New York, 1998. (b) Tour, J. M. *Trends Polym. Sci.* **1994**, *2*, 332.
(40) (a) Ho, K. S.; Bartus, J.; Levon, K.; Mao, J.; Zheng, W. Y.; Laakso, J.; Taka, T. *Synth. Met.* **1993**, *55*, 384. (b) Faid, K.; Frechette, M.; Ranger, M.; Mazerolle, L.; Levesque, I.; Leclerc, M.; Chen, T.-A.; Rieke, R. D. *Chem. Mater.* **1995**, *7*, 1390.

Table 5. Pitch and Roll Angles and Distances for Oligomers that Crystallize with a Dimer Motif[a]

compd	d_1	d_{p1}	d_{r1}	d_2	d_{p2}	d_{r2}	d	d_p	d_r	d_{tot}	N[b]	z (Å)[c]	$\Delta\%$
RT-B2T3+	3.47	2.41	0.20	3.47	2.41	0.20	6.95	4.82	0.40	4.84	34.8	8.46 (c)	0.3
LT-B2T3+	3.40	3.20	0.49	3.40	2.16	−0.22	6.80	5.36	0.27	5.37	38.3	8.66 (a)	0.1
DNT3	3.74	2.42	0.51	3.47	2.83	0.79	7.17	5.25	1.30	5.41	37.0	8.98 (a)	0.3
DCMT3	3.61	−3.32	0.48	3.50	5.70	0.40	7.11	2.38	0.88	2.54	19.4	7.54 (b)	0.1
BMSP	3.50	3.78	0.43	3.50	−0.75	1.57	7.00	3.07	2.00	3.66	36.6	7.93 (a)	1.4
SPSP	3.38	−6.72	1.70	3.38	9.48	0.87	6.76	2.76	2.57	3.77	29.2	7.74 (b)	0.1
UPSP	3.38	1.38	0.96	4.05	−0.83	11.6	7.43	0.55	12.5	12.5	59.3	14.55 (c)	0.1
UESP	3.37	3.51	1.29	3.37	1.42	0.84	6.73	2.09	2.13	2.98	23.9	7.36 (b)	0.3
T-av[d]	3.54	2.68	0.40	3.45	2.47	0.26	6.97	5.14	0.66	5.20	36.7		
P-av[e]	3.42	0.19	1.14	3.42	3.38	1.09	6.83	2.64	2.23	3.47	29.9		

[a] See Scheme 2 and the text for the definitions of the terms. All distances, d, are in Å. [b] $\cos(N) = d_{tot}/z$. [c] Letter in parentheses represents the crystallographic stacking axis. [d] Average of the thiophene values. [e] Average of the pentacene values, excluding the values for **UPSP**.
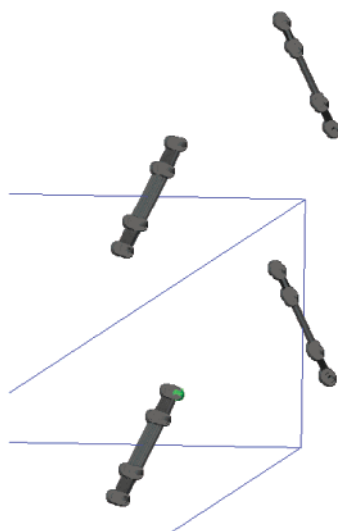

Figure 1. View down the long molecular axis of pentacene molecules packed in the "herringbone" structure. The "stacking axis" is vertical.

the nautical terms. Figure 2 shows the definitions of the pitch and roll angles. Let the $x-y$ plane be parallel to the molecular plane of a molecule in a π-stack. The vectors, x and y, represent the short and long axes of the molecule, respectively, and they are perpendicular to each other. The shortest distance between the planes of the two adjacent molecules in the π-stack is defined by a vector, d, which is perpendicular to the molecular plane (Figure 2). The crystallographic stacking direction is identified by a vector, z, that connects identical parts of the two adjacent molecules. The pitch angle (P) is used to assess the molecular slipping along the long axis and is defined as the angle between z_l (the projection of z on the $d-y$ plane) and the vector, d. The slip distance along the long molecular axis ("pitch distance") is:

$$d_p = |d| \tan P \quad (1)$$

In the same way, the slip of the molecules along the short molecular axis is determined by the roll angle (R), the angle between z_s and d. The vector, z_s, is the projection of z on the $d-x$ plane. The slip distance along the short molecular axis ("roll distance") is:

$$d_r = |d| \tan R \quad (2)$$

and the total slip distance, d_{tot}, is:

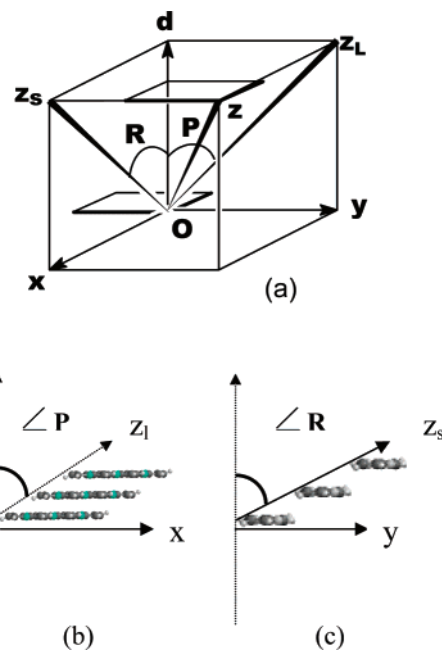$$d_{tot} = (d_p^2 + d_r^2)^{1/2} \quad (3)$$

Figure 2. (a) Definition of pitch P and roll R angles and associated distances and vectors. The labels x and y refer to the directions of the short and long molecular axes, respectively. (b) View along the short molecular axis of a "pitched" π-stack. (c) View along the long molecular axis of a "rolled" π-stack.

The crystallographic repeat distance, z, in the stack direction is given by

$$z = (d_p^2 + d_r^2 + d^2)^{1/2} = d(1 + \tan^2 P + \tan^2 R)^{1/2} \quad (4)$$

Note that the crystallographic axis z is greater than or equal to the π-stacking distance d, i.e., $z \geq 3.4-3.6$ Å, and z will increase as pitch or roll displacements increase.

When P or R is 45°, the corresponding slip distance is equal to d, which is typically about 3.5 Å, a distance slightly larger than the diameter of a benzene or thiophene ring. Therefore, if a π-stack undergoes a pitch angle distortion of 45°, then adjacent molecules slide along their long axes a distance of about 3.5 Å, leaving the "remainder" of the molecular π-systems of adjacent molecules still "overlapping" (Figure 2b). However, if the distortion is a roll angle of 45°, then the adjacent molecules slide completely out from under one another and there is little remaining π-overlap between them (Figure 2c). Thus, the degree of π-overlap between adjacent molecules depends critically on the nature and degree of the angular distortions of the molecular stack. Pitch angle distortions typically retain large intermolecular
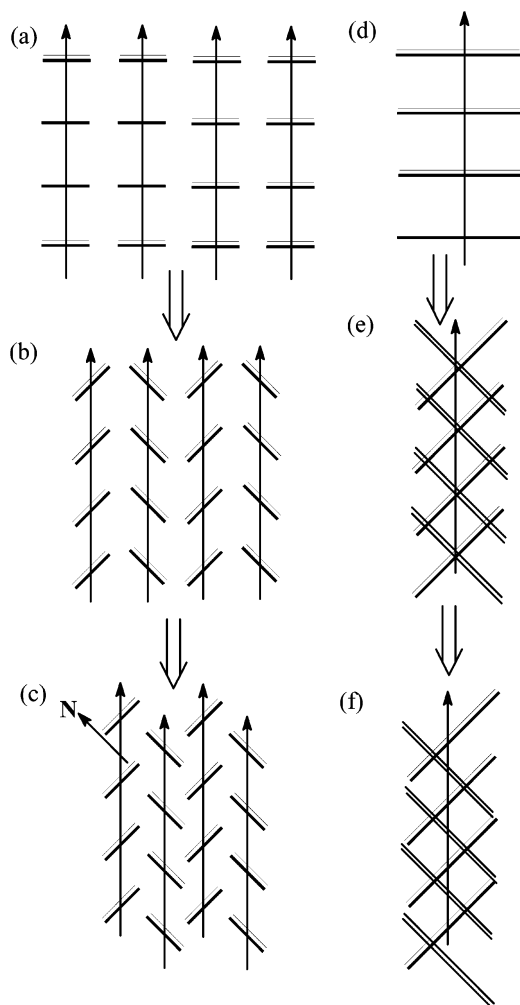
Figure 3. (a–c) Evolution of the herringbone structure (view down the long molecular axis) from (a) cofacial π-stacks, (b) through "rolled" π-stacks with no vertical displacement, to the final herringbone pattern (c) with vertical translations of alternate stacks by half the length of the stacking axis. (d–f) Evolution of a similar π-stacked structure: (d) view down the short axis molecular axis, i.e., perpendicular to the view as in a, (e) π-stacks "pitched" in opposite directions with no vertical displacement, and (f) displacements of alternate π-stacks (light and dark) by half the length of the stacking axis.

spatial overlaps, whereas roll angle inclinations ≥45° essentially destroy overlap between the π-orbitals of adjacent molecules.

The herringbone structure is produced when two adjacent stacks "roll" in the opposite direction, and the alternate stacks are then translated by half a unit cell length along the stack direction (see Figure 3). As shown by the view normal to the molecular plane (vector N in Figure 3c), there is minimal π-overlap in the herringbone structure. In fact, the largest intermolecular interactions occur between molecules in adjacent stacks ("diagonal interaction"), rather than between molecules in the same stack. One may also note the increase in packing efficiency afforded by the herringbone structure (Figure 3c) vis-à-vis the cofacial π-stack (Figure 3a).

Adjacent stacks may "pitch" in opposite directions, just as adjacent stacks in the herringbone "roll" in the opposite sense. Figure 3d represents the stacks of molecules depicted in Figure 3a as seen along the short molecular axis. Figure 3e represents the tilting of the molecules in alternate stacks, one behind the other, in opposite directions, indicated by dark and light lines. If the alternate stacks are now translated by one-half the stacking
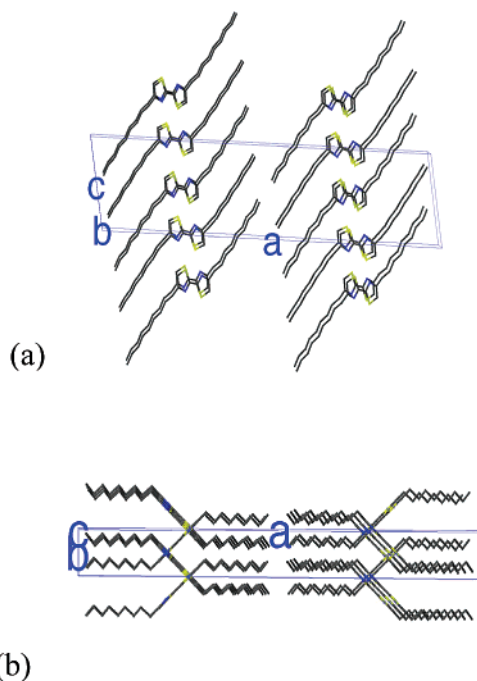
Figure 4. (a) **NBTz** molecular packing as viewed down the crystallographic *b*-axis, i.e., parallel to the π-stacking axis. (b) View parallel to the crystallographic *c*-axis, i.e., perpendicular to the π-stacking axis and approximately along the short molecular axis (see text).

distance, the structure depicted in Figure 3f is obtained. As with the herringbone structure, the packing density of the "alternating-pitch" structure is also greater than the undistorted "on-top" or cofacial π-stacked packing.

We define the angle N to be the angle between the stacking vector, z, and the normal to the molecular plane, d. In terms of the previously defined pitch and roll angles,

$$\cos(N) = d/z = (1 + \tan^2 P + \tan^2 R)^{-1/2} \quad (5)$$

The values of N, along with the measured pitch and roll angles and the slip distances of the structures discussed in this paper, are collected in Tables 2–5. The tables also show the value of z calculated using eq 4 and a comparison of z with the actual crystallographic stacking axis. The notion of "long" and "short" molecular axes is intuitively obvious but often lacks an unequivocal definition with molecules of different symmetry. For thiazole and thiophene oligomers with an even number of all-transoid rings, the long axis is essentially collinear with the central C–C bond. For oligoacenes, the long axis was taken to be the vector between the midpoints of the terminal C–C bonds. For the terthiophenes described here, we took the long axis to be the line connecting the terminal (5,5″) C-atoms. Since these definitions are not crystallographically mandated, and since there was some error in the measurement of the pitch or roll angles or slip distances, we use the "error" in the calculated stacking axis (eq 4) to determine the self-consistency of the measured pitch and roll parameters. The errors, expressed as Δ% and defined below, were generally less than 1%.

$$\Delta\% = \frac{|z| - |\text{axis}|}{|\text{axis}|} \times 100\% \quad (6)$$

Crystal Structures of NBTz and NBTh. The packing patterns of several representative conjugated oligomers will now
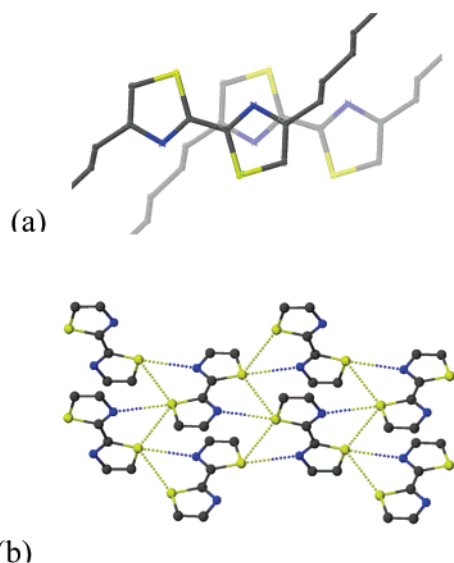
(a)

(b)

Figure 5. (a) View of two adjacent **NBTz** molecules in a π-stack, as seen perpendicular to the molecular plane. The plane of the darker molecule is 3.45 Å above the half-tone molecule. (b) Short intermolecular contacts between alternate π-stacks: S−S = 3.49 Å, S−N = 3.23 Å. In this figure, the crystallographic b-axis is approximately vertical and the c-axis is horizontal.

be presented. **NBTz** and **NBTh** crystallize in the $C_{2/c}$ and $P2_1/c$ space groups, respectively. **NBTz** has four molecules per unit cell, whereas **NBTh** has two molecules per unit cell. All the molecules lie on inversion centers, so the two rings are strictly coplanar in both compounds. Figure 4a shows a view of the packing of nonyl bithiazole, **NBTz**, molecules as seen down the crystallographic b-axis, which is the π-stacking axis. It is somewhat surprising that a lamellar structure is already produced at such a low "degree of polymerization". As viewed in Figure 4a, the molecules are tilted with respect to the viewing axis as shown in Figure 4b, a perspective that is at right angles to that in Figure 4a. The molecules are primarily tilted about their short axes, i.e., these molecules are "pitched" with respect to the stacking axis. The pitch angle, P, is 41.5°, and the interplanar spacing, d, is 3.45 Å, so the slip distance along the long molecular axis is $d_p = 3.05$ Å. The molecules have a modest roll angle, $R = 14.3°$, corresponding to a side slip $d_r = 0.88$ Å. The effect of these slip distances on the positions of adjacent molecules in the π-stack may be seen in Figure 5a, a view normal to the molecular plane. The packing arrangement of **NBTz** is thus derived as depicted in Figure 3d−f.

The packing motif in which the two molecules in the unit cell pitch in opposite directions also gives rise to close contacts between molecules in adjacent π-stacks as illustrated in Figure 5b. The dotted lines show the short contact distances, $d_{S−S} = 3.49$ Å and $d_{S−N} = 3.23$ Å. In terms of close intermolecular contacts between atoms in the conjugated backbone, the molecules of NBTz are packed into 2-D sheets parallel to the (100) planes. In the direction of the b-axis, the molecules are π-stacked, and adjacent π-stacks are "stitched together" along the c-axis via the short S−S and S−N contacts. Thus, we might expect a 2-D character to charge or energy transport in **NBTz** crystals.

The structure of nonyl bithiophene, **NBTh**, presents a striking contrast to that of the bithiazole analogue. At first glance, the structure appears similar to that of **NBTz**, but the alkyl side
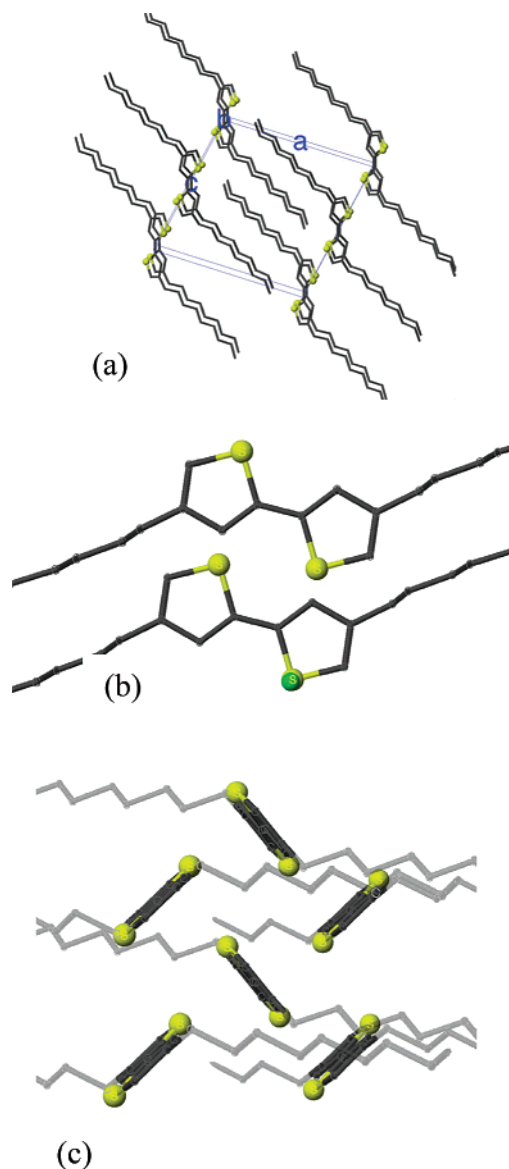

(a)

(b)

(c)

Figure 6. (a) View of the packing in **NBTh**, as seen down the b-axis. This illustration shows 12 molecules, stacked two deep. (b) View normal to the molecular plane (the two molecules are separated vertically by a distance of 3.36 Å). (c) View down the long molecular axes (parallel to the (−4 0 2) planes).

chains are interdigitated (Figure 6a). It is interesting to note that Prosa et al. have recently reported a polymorph of poly-(3-dodecylthiophene) with interdigitated side chains.[41] Unlike the structure of **NBTz**, the molecules of **NBTh** are rotated about the long molecular axis, giving a large roll angle, $R = 47.9°$, but the structure has a very small pitch angle, $P = 2.6°$. As a consequence, the adjacent molecules of **NBTh** slide sideways with respect to each other a distance of 3.72 Å, such that when viewed normal to the molecular plane, there is no spatial overlap of the π-systems on adjacent molecules (Figure 6b). When viewed down the long molecular axis, the main chains appear to be stacked in a herringbone-like pattern (Figure 6c). The difference between the packing as seen in Figure 6c and a true herringbone packing is that the alternate vertical columns of main chains as seen in Figure 6c are translated out of the plane

(41) Prosa, T. J.; Winokur, M. J.; McCullough, R. D. *Macromolecules* **1996**, *29*, 3654.

of the paper by a distance corresponding to $c/2$, whereas they would all lie in the same plane in a true herringbone pattern. (The view in Figure 6c contains the six, leftmost molecules shown in Figure 6a, as seen along the central C–C bond axis.) The angle between the planes of the molecules in translationally nonequivalent stacks is $2N = 95.8°$, as calculated by eq 5.

Crystal Structure of EBTz. The structure of **EBTz** was determined in order to see the effect of changing the length of the alkyl side chain on the details of the molecular packing. **EBTz** crystallizes in the $P2_1/n$ space group with two independent molecules per unit cell with each molecule on an inversion center, making the two rings coplanar. The π-stacking axis in **EBTz** is the a-axis (Figure 1S, Supporting Information), rather than the b-axis as in **NBTz**, and the interplanar distance between molecules in a π-stack is $d = 3.67$ Å, slightly larger than in **NBTz**. The molecules in the π-stacks are canted relative to the stacking axis by $N = 45.1°$ (Figure 1S). The pitch angle P is 42.6°, and the roll angle R is 21.9°, giving the "staircase" structure similar to that of **NBTz** (Figure 2Sa) with $d_p = 3.37$ Å and $d_r = 1.47$ Å, about half the width of the thiazole ring, 2.46 Å. The closest contact distances within the π-stack are C–C, 3.66 Å; C–N, 3.79 Å; and S–N, 3.89 Å, while the short contacts between the translationally nonequivalent molecules are C–N, 3.96 Å, and C–C, 4.08 Å (Figure 2Sb). These distances suggest a weaker interaction between the translationally nonequivalent molecules as compared with the interactions in **NBTz**. The shorter intermolecular contact distances in **NBTz** may be the result of the crystallization of the long alkyl side chains, an effect that has been noted to result in greater crystallinity and better charge transport properties in regioregular poly(3-alkylthiophene)s.[27,40]

Crystal Structure of EBTz2. Figure 7 displays the packing of the **EBTz2** molecules. There are four molecules per unit cell in the $C2/c$ space group, and each molecule is located on an inversion center. The inner rings are strictly coplanar, and the outer rings are twisted slightly out of planarity with respect to the inner rings by about 3°. Thus, the solid-state packing provides nearly maximal overlap of π-orbitals among all the rings in a given molecule. The molecules are π-stacked along the crystallographic b-axis with an interplanar distance $d = 3.48$ Å. As viewed in Figure 7b, the stacks are canted relative to the stack axis with $N = 48.5°$.

The pitch angle, $P = 48.0°$, gives the molecules a staircase structure similar to **NBTz** or **EBTz**. The slip distances are $d_p = 3.86$ Å, nearly a one-ring-length displacement (the length of **EBTz2** is 13.9 Å), and $d_r = 0.75$ Å due to a roll angle $R = 12.1°$. Therefore, there remains substantial spatial overlap between adjacent molecules (Figure 8a). The shortest distances within the π-stack are C–C, 3.54, 3.63, and 3.69 Å; C–S, 3.57, 3.64, and 3.76 Å; C–N, 3.59 Å; and S–N, 3.60 Å, while the shortest distances between a molecule in one stack and a molecule in an adjacent stack are S–S, 3.51 Å; S–N, 3.54 Å; C–N, 3.61 Å; and C–S, 3.80 Å (Figure 8b).

Crystal Structure of EBTz-COOH. This compound crystallizes in the $C2/c$ space group with eight independent molecules per unit cell. The molecules surround inversion centers located between the carboxylic acid groups. The substituted ring is twisted slightly out of planarity with respect to the adjacent ring by nearly 4°. As with **EBTz2**, the molecules are π-stacked ($d = 3.42$ Å) along the direction of the b-axis. The presence of
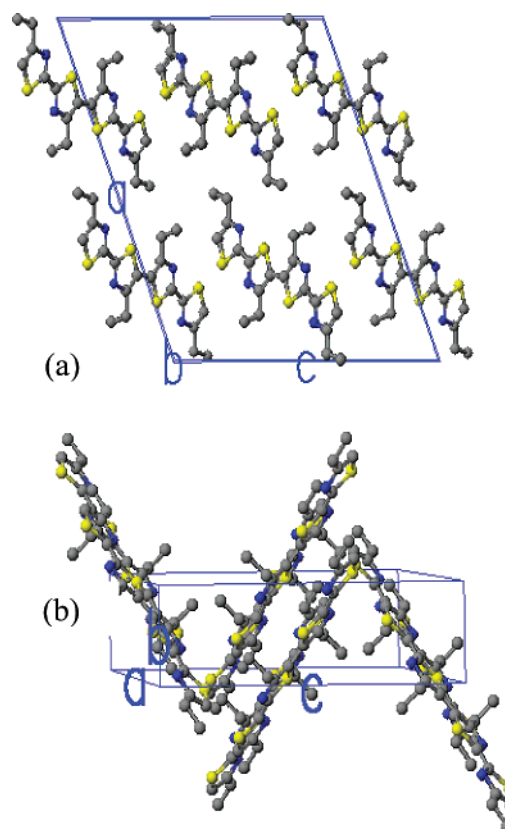
Figure 7. Illustration of the crystal unit cell of **EBTz2**: (a) view down the b-axis; (b) view perpendicular to the b-axis.
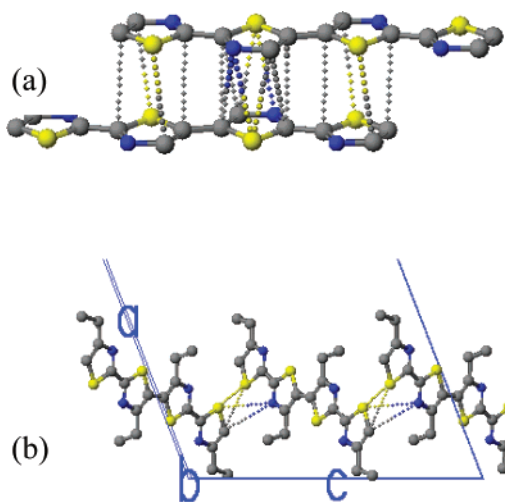

Figure 8. (a) Illustration of the short contacts between **EBTz2** molecules within a π-stack and (b) between adjacent π-stacks.

the terminal carboxylic acid groups on the bithiazole rings in **EBTz-COOH** leads to inter-π-stack H-bonding (O··O distance = 2.64 Å), such that the H-bonded dimer behaves like a single four-ring oligomer in the solid state. Indeed, the packing and pattern of short contacts in **EBTz-COOH** closely resembles those shown for **EBTz2** in Figures 8 (see Figures 3S and 4S). Interstack short-contact distances link the π-stacks into 2-D sheets parallel to the $(10\bar{1})$ planes with $N = 48.2°$.

The pitch angle, P, in the **EBTz-COOH** π-stacks is 47.3°, resulting in a staircase structure with $d_p = 3.71$ Å, a slip distance about half of the length of the molecule (7.6 Å). The roll angle $R = 15.4°$, and $d_r = 0.94$ Å, about one-third of the width of the

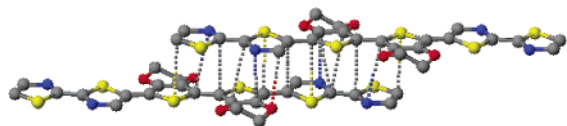**Figure 9.** Illustration of short contacts between adjacent molecules within a given π-stack in **BT$_2$B**.

bithiazole ring. This slip distance aligns the carbonyl groups on adjacent molecules in the stack in a favorable, head-to-tail orientation (Figure 4S). The shortest contact distances within a given π-stack are C–C, 3.25, 3.43, and 3.62 Å; C–O, 3.45 and 3.54 Å; N–O, 3.35 Å; C–S, 3.59, 3.63 Å; and S–N, 3.63 Å. There are also short distances between one dimer-like unit and the unit in adjacent π-stacks: S–S, 3.52 Å; S–N, 3.91 Å (Figure 4S).

Crystal Structure of BT$_2$B. This compound crystallizes in the $P_{2(1)/n}$ space group with $Z = 2$. Each molecule lies on an inversion center, and the five-membered rings of the (EDOT)$_2$ groups are strictly coplanar. The two outer bithiazole rings are twisted at a 4.5° angle from the EDOT thiophene rings. However, the C$_4$O$_2$ ring of EDOT is ruffled. Within a given stack, the molecules are aligned in a slipped π-stack along the direction of the b-axis with $d = 3.50$ Å (Figure 5Sa). As viewed perpendicular to (10$\bar{1}$) plane, the translationally nonequivalent stacks are canted with respect to each other with $2N = 138.0°$ (Figure 5Sb). The pitch angle, P, is 69.0°, and this value is much larger than the pitch angles (ca. 45°) in the previously discussed bithiazole structures. The large pitch angle gives a large slip distance $d_p = 9.25$ Å, i.e., the length of about three thiazole rings. This large slip distance places a bithiazole ring (acceptor) of one molecule over the (EDOT)$_2$ group (donor) of the adjacent molecule in the π-stack. The large pitch angle in **BT$_2$B** may be attributed to a favorable interaction between the bithiazole group (acceptor) and the EDOT group (donor) of the adjacent molecules. The roll angle is 8.2°, resulting in a short-axis slip distance $d_r = 0.51$ Å, thus maintaining substantial spatial overlap between the adjacent π-systems within a π-stack. The short contacts within a given π-stack are C–C, 3.55, 3.58, and 3.60 Å; C–N, 3.45 and 3.69 Å; C–O, 3.35 Å; and C–S, 3.55, and 3.58 Å (Figure 9). The short contacts between a molecule in one stack and a molecule in an adjacent stack are C–N, 3.52 Å; C–C, 3.84 Å (Figure 6S).

Other Bithiazole Oligomers. The structures of several other bithiazole oligomers have been reported recently. The bithiazole dimers, **3P2** and **3H2**,[19] and the bis(bithiazole)diacetylene, **BBD** (Scheme 1),[34] have structures that closely resemble that of **EBTz** with large pitch angles near 40–45° and smaller roll angles 12–25°, thus maintaining substantial spatial overlap between adjacent molecules in the π-stack. The structures of **BBD** and **BT$_2$B** show that the typical π-stacked packing for bithiazoles is maintained even when the bithiazole groups are separated by intervening groups, e.g., EDOT or ethynyl.

Thiophene Oligomers. The structures of several representative thiophene oligogomers have been analyzed with the methods described above. The results are collected in Table 3. Unsubstituted sexithiophene exists in two polymorphs, $P2_1/n$ and $P2_1/a$, labeled **T6-n** and **T6-a**, respectively.[21,22] The π-stacking of the two polymorphs is quite different. In the **T6-a** structure, $P = 0.0°$, but $R = 60.7°$, giving $d_p = 0.0$ and $d_r = 4.98$ Å, whereas in the **T6-n** structure, $P = 41.3$, $R = 58.4$, $d_p = 2.50$ Å, and $d_r = 4.64$ Å. Since both structures have large

Figure 10. Packing of molecules of **B2T3** as seen down the long molecular axis. The stacking direction is vertical in the picture, and the herringbone-like structure occurs in pairs of stacks to give a "lamellar herringbone" structure.

roll angles, both have a herringbone-like structure in that adjacent molecules in a stack slip out from under each other, but the **T6-n** structure has an appreciable pitch distance as well.

Lateral alkyl groups are expected to disrupt the herringbone packing pattern because a strictly edge-to-face packing is not possible if long alkyl side chains are present. It is therefore a bit surprising to see that, with one exception (**PFT6**), all the thiophene oligomers in Table 3 crystallize with large roll angles typical of the herringbone structure, even though there are alkyl side chains present. Dibutyl- and tetrahexylsexithiophene, **B2T6** and **H4T6**, respectively, crystallize with a pseudoherringbone structure with interdigitated side chains in structures that are very similar to that of **NBTh** described above.[42,43] Within a given stack, there are large roll displacements, $d_r = 4.90$ and 3.45 Å, respectively. Increasing the number of alkyl side chains seems to promote a larger pitch angle. Thus, the structure of tetrahexylsexithiophene, **H4T6**, has an appreciable pitch angle ($P = 33.9°$), but **B2T6** has a very small pitch angle, $P = 2.1°$. Oligomers with geminally disubstituted thiophene rings may show a different type of "lamellar herringbone" structure, as seen in Figure 10 for **B2T3**.[44] This structure has herringbone-like stacks that are arranged in layers separated by the alkyl side chains. In all these thiophene structures, the large roll displacements give rise to structures with essentially no π-overlap between adjacent molecules in a stack. The only structure listed in Table 3 that does not have a large roll displacement is that of perfluorosexithiophene, **PFT6**.[45] In this structure, the molecular packing is very similar to that of **EBTz2**, although the roll displacement of the thiophene is still larger than that of the thiazole, 1.36 vs 0.75 Å.

Pentacenes. Table 4 lists the structural parameters of three pentacenes. The unsubstituted parent, **PENT**, has a typical herringbone structure with $d_p = 2.10$ Å and $d_r = 5.35$ Å.[20] **TBP** and **TMSP** have two *tert*-butylethynyl or two trimethylsilyl-ethynyl groups symmetrically attached to the central ring (see Scheme 1).[46] The compounds each crystallize in π-stacks with modestly large pitch displacements, $d_p = 5.48$ and 4.55 Å, respectively, and small roll displacements, $d_r = 0.87$ and 1.17 Å, respectively. Thus, the parent pentacene has no π-overlap

(42) Herrema, J. K.; Wildeman, J.; van Bolhuis, F.; Hadziioannou, G. *Synth. Met.* **1993**, *60*, 239.
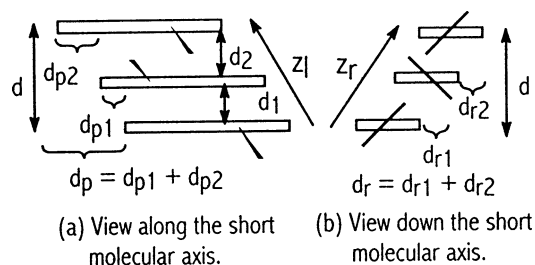(43) Destri, S.; Ferro, D. R.; Khotina, I. A.; Porzio, W.; Farrina, A. *Macromol. Chem. Phys.* **1998**, *199*, 1973.
(44) Graf, D. D.; Duan, R. G.; Campbell, J. P.; Miller, L. L.; Mann, K. R. *J. Am. Chem. Soc.* **1997**, *119*, 5888.
(45) Sakamoto, Y.; Komatsu, S.; Suzuki, T. *J. Am. Chem. Soc.* **2001**, *123*, 4643.
(46) Anthony, J. E.; Eaton, D. L.; Parkin, S. R. *Org. Lett.* **2002**, *4*, 15.

Scheme 2

(a) View along the short molecular axis.

(b) View down the short molecular axis.

between adjacent molecules, but the substituted structures have appreciable overlap, as was pointed out by Anthony et al.[46,47]

Dimeric Structures. There are several structures of conjugated oligomers that are based on packing of dimers. This results when the crystallographic repeat distance in the stack direction is doubled because of packing constraints caused by alternating side chains or rings twisted out of planarity (see Scheme 2). The analysis in terms of pitch and roll can still be applied to these dimer structures. There are now two sets of pitch and roll displacement parameters, one for each pair of molecules in the stack. Each of the displacements, d_{p1}, d_{p2}, etc., as well as the overall displacements, $d_p = d_{p1} + d_{p2}$ and $d_r = d_{r1} + d_{r2}$, have the same relationships to their respective distortion angles, etc., as described by eqs 1−5. The values of the displacement parameters are listed in Table 5 for several structures of interest.

The first two structures described in Table 5 are the monocations (as the PF_6^- salts) of the terthiophene, **B2T3**, shown in Scheme 1. These cations crystallize in two polymorphs, the room-temperature (**RT-B2T3**) and low-temperature (**LT-B2T3**) forms.[44,48] As described above (Figure 10), the neutral **B2T3** has a lamellar herringbone packing, but each of the oxidized forms has a π-stacked structure that is characterized by small roll displacements between adjacent molecules, $d_r = 0.2-0.5$ Å. The pitch displacements are in the range $d_p = 2.2-3.2$ Å, which leaves a large spatial overlap between adjacent molecules in the π-stack as pointed out previously.[44] In their report, Graf et al. describe the structure of **LT-B2T3** as consisting of dimers with different d spacings, d_1 and d_2. Indeed, d_1 and d_2 are not equal if one uses the mean plane of all the atoms in the three thiophene rings. However, the reason the z-axis is doubled is that the central thiophene ring is twisted out of planarity in the manner depicted in Scheme 2. Using all the atoms represented in Scheme 2 to generate a mean plane decreases d_1 and increases d_2. In the analysis reported here, the mean planes were generated only from the planar, terminal thiophene rings with the result that the interplanar distances are equal (i.e., $d_1 = d_2$), but the distances are contracted in the low-temperature polymorph, from 3.47 to 3.40 Å. In any event, oxidation causes a dramatic switch from a R-dominated, herringbone-like packing to the P-type, π-stacked motif. Placing nitro groups on the terminal thiophene rings (**DNT3**) also drives the packing into the π-stacked morphology as shown by the small roll displacements in Table 5.[49]

The remaining four entries in Table 5 are all substituted pentacenes. The unsymmetrically substituted derivatives, **UP-**

SP[50] and **UESP**,[46] form dimer structures as a result of the alternating placements of the side chains as depicted in Scheme 2a. In **UPSP**, the large size of the $^iPr_3Si$ groups drives such a large roll distortion in d_{r2} that the dimers are effectively separated and there are no extended π-contacts in the crystal. **UESP** has roll displacements of less than 1.3 Å and pitch displacements of about 3.4 Å, giving a π-stacked structure with the π-stacks isolated by the intervening triethylsilylethynyl side chains. Although π-stacked, both **BMSP** and **SPSP** have at least one relatively large roll displacement in the range 1.6−1.7 Å.

Discussion

A new phenomenological description of the solid-state packing of conjugated oligomers has been developed that uses "pitch" (P) and "roll" (R) inclinations from an idealized cofacial π-stack to describe the solid-state packing. Pitch distortions slide adjacent molecules relative to one another in the direction of the long molecular axis, whereas roll inclinations produce a "sideways" slip along the short molecular axis. Pitch distances are typically shorter than the molecular length, leaving substantial spatial overlap between adjacent molecules in the π-stacks. Roll distortions are often larger than the molecular width and destroy spatial and orbital overlap between adjacent molecules. Analyzed in this manner, the "herringbone" and "π-stack" structures are seen to be closely related and differ primarily in the major slip direction.

Solid-state packing of conjugated compounds have been analyzed previously by Kitaigorodsky and by Desiraju and co-workers, among others. Kitaigorodsky showed that minimization of sums of transferable atom−atom pairwise potentials could be used to predict structures within a limited range.[51] Desiraju classified aromatic hydrocarbon structures into four types: herringbone (HB), dimer-based, sandwich herringbone (SHB), a "flattened herringbone" called "γ", and on-top, π-stacked "β" structures.[52,53] These four types were characterized by the length of the short crystallographic axis and the angle between the planes of adjacent (nontranslationally equivalent) molecules. Structures identified as β have one very short axis, ~4.0 Å; γ structures have a short axis in the range 4.6−5.4 Å, and HB structures are characterized by short axes in the range 5.4−8 Å. The SHB structure basically doubles the stacking axis. Gavezzotti and Desiraju[53] also defined the two vectors R_{IP} and R_N. R_{IP} is identical to the interplanar vector, $d = O_1O_2$ (Figure 2), used in this work, and R_N is a vector that connects the center of masses of nearest neighbor molecules. They further define an angle $\alpha = \cos^{-1}(R_{IP}/R_N)$. In γ and β structures, $R_{IP} = d$ (as defined here) and $R_N =$ the stacking vector (z), so that α is equivalent to N for these structures; however, in the HB structure, R_N connects neighboring molecules in adjacent stacks and the significance of α is not clear.

The system of classification presented in this paper is further related to Desiraju's nomenclature as follows: As eq 4 shows, as the pitch and roll angles, P and R, approach zero, the stacking (short crystallographic) axis, z, approaches the interplanar

(47) Haddon, R. C.; Chi, X.; Itkis, M. E.; Anthony, J. E.; Eaton, D. L.; Siegrist, T.; Mattheus, C. C.; Palstra, T. T. M. *J. Phys. Chem. B* **2002**, *106*, 8288.
(48) Graf, D. D.; Campbell, J. P.; Miller, L. L.; Mann, K. R. *J. Am. Chem. Soc.* **1996**, *118*, 5480.
(49) Pappenfus, T. M.; Raff, J. D.; Hukkanen, E. J.; Burney, J. R.; Casado, J.; Drew, S. M.; Miller, L. L.; Mann, K. R. *J. Org. Chem.* **2002**, *67*, 6015.

(50) Anthony, J. E.; Brooks, J. S.; Eaton, D. L.; Parkin, S. R. *J. Am. Chem. Soc.* **2001**, *123*, 9482.
(51) Kitaigorodskii, A. I. *Molecular Crystals and Molecules*; Academic Press: New York, 1973.
(52) Desiraju, G. R. *Crystal Engineering, The Design of Organic Solids*; Elsevier: New York, 1989.
(53) (a) Gavezzotti, A.; Desiraju, G. R. *Acta Crystallogr. B* **1988**, *44*, 427. (b) Desiraju, G. R.; Gavezzotti, A. *Acta Crystallogr. B* **1989**, *45*, 473.

stacking distance $d \approx 3.6$ Å. This situation corresponds to the β structure. As the angles P or R increase, the length of the crystallographic stacking axis (short axis) increases. Since an increase in *either* P or R inclinations causes the stacking axis to increase, the P/R classification says more about the molecular packing than a scheme based solely on the size of the short molecular axis. The γ structure typically corresponds to a structure with $d_r <$ ca. 2 Å and a total slip distance (d_{tot} of eq 3) of 3.0–4.1 Å and is common in disc-shaped aromatics, e.g., perylenes or porphyrins. The HB structure occurs with predominately R-displaced packing ($d_r > 3.5$ Å) with d_{tot} of 4.1–7 Å. Unlike the pitch and roll parameters described in this paper, the parameters R_{IP}, R_N, and α do not have a general connection to the short cell axis (stacking axis). As the data in Table 5 show, structures based on packing of dimers can occur with either pitch or roll inclinations. Thus, the present classification of structures is both more generally applicable and more directly related to the details of the molecular packing than the earlier classifications.

The most striking aspect revealed by the present analysis is the huge difference in packing preferences between oligomeric thiazoles and thiophenes. Thiazole oligomers typically have pitch displacements, $d_p = 3$–4 Å, and small roll displacements, $d_r <$ 1.5 Å, that allow neighboring molecules to maintain considerable spatial overlap. This packing motif may be called "π-stacked". Conversely, thiophene oligomers have small pitch displacements, $d_p < 2.5$ Å, and large roll distances, $d_r > 3.5$ Å, which defines the herringbone packing and effectively destroys π–π overlap between adjacent molecules in the stacking direction. In these herringbone structures, the largest intermolecular interactions are between neighboring molecules in adjacent stacks (diagonal interactions). Unsubstituted pentacene also has a large roll displacement that destroys π-overlap within the stack, but the substituted pentacenes of Anthony et al. seem to have either π-stacked structures (Table 4) or dimer-based structures intermediate between the herringbone and the π-stack, i.e., the dimers have at least one roll displacement in the range $1.3 < d_r < 2$ Å as well as at least one large pitch distance, $d_p > 3.5$ Å. The dimer structures arise from packing constraints of the side chains or nonplanarity in the main chains. Thus, of the compounds surveyed here, thiazoles show the strongest preference for π-stacking, even when other groups, e.g., dithienyl or diethynyl, are incorporated into the molecule (cf. **BT₂B** and **BBD**, Table 2).[54]

Transport Properties and Molecular Packing. From the standpoint of increasing charge carrier mobility by generating large valence or conduction bandwidths (proportional to the orbital overlaps of adjacent molecules) in crystalline conjugated oligomers, it would seem that crystals with π-stacked molecules would be better than those with herringbone packing. Also, from the standpoint of the hopping theory of electron conduction, π-stacks would also lead to higher mobility because the hopping rate decreases exponentially with the hop distance and increases with intermolecular orbital overlap.[13,55] Experimental evidence

that π-stacked structures can have higher mobilities than herringbone-structured solids is still scant, however.

The highest FET carrier mobility reported to date, ca. 1.5 cm² V⁻¹ s⁻¹, for an undoped organic material was measured for pentacene, a herringbone-structured solid.[7] However, to get this high mobility, the pentacene must be repeatedly purified by gas transport, and great care must be taken to ensure proper film growth, morphology, and electrode contact. More typical mobility values for "off-the-shelf" pentacene FETs are in the range 0.01–0.1 cm² V⁻¹ s⁻¹. In contrast, relatively high mobilities have been reported for compounds that have a higher degree of intermolecular overlap, even without the stringent purifications required for high-mobility pentacene. Torrent et al. reported that FETs constructed with solution-cast **DT-TTF** (Scheme 1, Table 3) as the active semiconductor had mobilities in the range 0.1–1.4 cm² V⁻¹ s⁻¹.[56] With a very small pitch distance, 0.12 Å, and a modest roll displacement of only 1.75 Å, adjacent molecules of **DT-TTF** retain appreciable π-overlap even though the packing was previously called a herringbone on the basis that $d_r > d_p$. (Note: the small total inclination produces a short axis distance, 3.99 Å, about equal to the molecular interplanar distance, i.e., this is a β structure in Desiraju's nomenclature.) Similarly, Katz et al. have reported high electron mobilities, $\mu \approx 0.2$ cm² V⁻¹ s⁻¹, for FETs with solution-cast, N-fluoroalkylated naphthalene tetracarboxylate as the semiconducting layer.[57] This disc-shaped molecule crystallizes in a γ-structure with the parameters, $d = 3.184$ Å, $P = 20.97°$, $R = 50.77°$, $d_p = 1.22$ Å, $d_r = 3.90$ Å, $N = 52.4°$, $z = b = 5.218$ Å. The width (C···C) of the molecule is 4.9 Å, so the large roll distance of 3.9 Å still leaves considerable intermolecular overlap in the stacking direction. Another π-stacked compound, **DCMT3** (Scheme 1, Table 5), crystallizes in a dimer motif due to the centrally substituted butyl groups on alternate molecules in the stack pointing in opposite directions. The small slip distances, $d_p < 5.7$ Å and $d_r < 0.9$ Å, leave good spatial overlap between adjacent molecules. This material had electron mobilities as high as 0.2 cm² V⁻¹ s⁻¹.[16b] Although the thin film structure is slightly different from the bulk, the molecules retain the π-stacked morphology.[16] The highest reported electron mobilities, up to 0.6 cm² V⁻¹ s⁻¹, were measured in an FET with bottom contact geometry for an *N,N'*-dioctylyl-1,2,7,8-perylenetetracarboxylate diimide.[58] The exact structure of the film is not known, but disc-shaped *N*-alkyl perylene diimides typically have the γ-structure with $d \approx 3.4$ Å, $d_p \approx 3$–3.5 Å, and $d_r \approx 1$ Å, i.e., there is substantial spatial overlap of neighboring π-systems. It might also be pointed out that FET mobilities measured with bottom contacts for source and drain electrodes are often an order of magnitude smaller than those measured with top contacts.[59]

Theory also supports the hypothesis that π-stacking may lead to higher carrier mobilities. Haddon et al.[47] have calculated the valence and conduction bandwidths of the pentacene derivatives, **TMSP** and **SPSP**, as well as the parent pentacene, by the Extended Hückel method. They found bandwidths ≤220 meV

(54) Presence of halogen substitution on aromatic molecules has also been recognized as favoring the formation of π-stacks. See Chapter 6 in ref 52 and: Sarma, J. A. R. P.; Desiraju, G. R. *Acc. Chem. Res.* **1986**, *19*, 222.

(55) (a) Marcus, R. A. *Rev. Mod. Phys.* **1993**, *65*, 599. (b) Sutin, N. In *Electron Transfer in Inorganic, Organic, and Biological Systems*; Bolton, J. R., Mataga, N., McLendon, G., Eds.; American Chemical Society: Washington, DC, 1991.

(56) Mas-Torrent, M.; Durkut, M.; Hadley, P.; Ribas, X.; Rovira, C. *J. Am. Chem. Soc.* **2004**, *126*, 984.

(57) Katz, H. E.; Lovinger, A. J.; Johnson, J.; Kloc, C.; Siegrist, T.; Li, W.; Lin, Y.-Y.; Dodabalapur, A. *Nature* **2000**, *404*, 478.

(58) Malenfant, P. R. L.; Dimitrakopoulos, C. D.; Gelorme, J. D.; Kosbar, L. L.; Graham, T. O.; Curioni, A.; Andreoni, W. *App. Phys. Lett.* **2002**, *80*, 2517.

(59) Meng, H.; Zheng, J.; Lovinger, A. J.; Wang, B.-C.; Van Patten, P. G.; Bao, Z. *Chem. Mater.* **2003**, *15*, 1778.

for pentacene, compared to values of 860 meV for the conduction band of **TMSP** and a 2-D band structure with widths of 330−360 meV for **SPSP**. The valence bandwidths of **TMSP** and **SPSP** are slightly smaller than those for pentacene. These calculations illustrate two points: (1) that π-stacked structures potentially have larger bandwidths than herringbone structures, and (2) that spatial overlap is a necessary but not sufficient condition for large orbital overlap. The necessary condition for orbital overlap in the π-stack is that $w/d_r \geq 1$, i.e., the width (w) of the molecule be greater than the roll displacement. However, the overlap of molecular *orbitals* on adjacent molecules depends on their nodal properties, as well as on their relative spatial arrangements, as recently emphasized by Brédas and co-workers.[60]

How can these insights be used to design high-mobility materials? The description of the nearest-neighbor packing of conjugated oligomers described in this paper is purely phenomenological. The basis of the different packing structures of, say, thiazoles and thiophenes, is not addressed. Many of these conjugated molecules are centrosymmetric and therefore do not have an electric dipole moment. Thus, the leading electrostatic term in the interaction potential is probably quadrupolar in nature.[61] It is to be noted that relatively small changes can flip a structure from herringbone to π-stacked, for example, compare **B2T3** (herringbone) with its π-stacked, dinitro derivative, **DNT3**, or its oxidized forms, **RT-B2T3**$^+$ and **LT-B2T3**$^+$ (Tables 3 and 5). The alignment of the nitro groups in **DNT3** resembles the overlap of the carboxyl groups in **EBTz-COOH** (Figure 4S), so that the attraction between local dipoles in the π-stacked structure seems to be the primary factor favoring the π-stacked structure over the HB in **DNT3**. Thus, placement of strongly polar groups in the α,ω-positions may promote π-stacking. Desiraju has previously pointed out that replacement of H- by Cl-atoms promotes π-stacking (the "halogen effect").[54] The partially filled band of oxidized (p-doped) materials would favor a structure that maximizes the band dispersion, i.e., the π-stack, because the bonding interactions of the electrons in the bottom half of the band are not completely canceled by the electrons in the top half of the band. Conversely, the filled band of neutral molecules favors structures with small dispersions such as, the herringbone. Thus, doping will promote π-stacking. It is interesting in this regard to note that the conductivities of around 1000 S/cm reported for p-doped HT-P3ATs imply mobilities of at least 50 cm^2 V^{-1} s^{-1}.[62] This large value suggests band-like transport and argues for appreciable intermolecular interaction, possibly via π-stacked crystalline domains.

Comparing the simple nonyl bithiophene and nonyl bithiazole structures, the ring H-atoms in the thiophene do not seem to be involved in any close contacts ($\leq$sum of van der Waal's radii, VDW) with neighboring molecules; however, the C(5)···S distance, 3.480 Å, between neighboring molecules in adjacent stacks is less than the sum of the VDW, and the direction of close contact has an edge-to-face orientation, suggestive of a relatively strong C$\alpha(\delta^-)$···S(δ^+) attraction. The interatomic approaches that are less than the VDW in nonyl bithiazole, S···N = 3.240 Å and S···S = 3.487 Å, are, in contrast, directed edge-to-edge. Do peripheral interactions influence the packing more than face-to-face forces in *both* herringbone and π-stacked structures? Having a convenient set of parameters such as those presented here with which to compare various packing motifs should aid the theoretical investigation of the factors that give rise to the preference of different classes of compounds for different types of structures. Such understanding would help in the design of wide-bandwidth materials for high carrier mobility applications, e.g., organic field effect transistors, OFETs. Future work will explore these questions.

Supporting Information Available: Table 1S listing crystallization conditions and crystallographic information files (CIF) for **NBTh**, **EBTz**, **EBTz-COOH**, **EBTz2**, and **BT₂B** and Figures 1S−6S, depicting various views of the crystal packing of bithiazole oligomers. This material is available free of charge via the Internet at http://pubs.acs.org.

JA0397916

(60) Bredas, J. L.; Calbert, J. P.; da Silva Filho, D. A.; Cornil, J. *Proc. Nat. Acad. Sci.* **2002**, *99*, 5804.
(61) (a) Hunter, C. A.; Sanders, J. K. M. *J. Am. Chem. Soc.* **1990**, *112*, 5525. (b) Hunter, C. A. *Angew. Chem., Int. Ed. Engl.* **1993**, *32*, 1584.
(62) (a) McCullough, R. D.; Tristram-Nagle, S.; Williams, S. P.; Lowe, R. D.; Jayaraman, M. *J. Am. Chem. Soc.* **1993**, *115*, 4910. (b) McCullough, R. D.; Williams, S. P. *J. Am. Chem. Soc.* **1993**, *115*, 11608. (c) Politis, J. K.; Nemes, J. Curtis, M. D *J. Am. Chem. Soc.* **2001**, *123*, 2537.